J. Condensed Matter Nucl. Sci. 5 (2011) 42–51

Research Article

Time-resolved Measurements of Loading Ratios and Heat Evolution in D_2 (and H_2)-Pd·Zr Mixed-oxide Systems

Akira Kitamura,* Yuki Miyoshi, Hideyuki Sakoh and Akira Taniike

Graduate School of Maritime Sciences, Kobe University, 5-1-1 Fukaeminani-machi, Higashinada-ku, Kobe 658-0022, Japan

Akito Takahashi, Reiko Seto and Yushi Fujita

Technova Inc., Uchisaiwaicho 1-1-1, Chiyodaku, Tokyo 100-0011, Japan

Abstract

Using a twin system for hydrogen absorption, we have studied heat evolution and high-energy particle generation by D_2 and H_2 gas absorption into nano-sized mixed oxide powders of palladium and zirconium. We have found very large energy of hydrogen absorption by Pd·Zr oxide compounds exceeding 1.0 eV/D (or H) together with a very high D/Pd loading ratio, exceeding 1.0. The system has been improved to enable time-dependent measurements of the gas flow rate and loading ratio simultaneously with the output heat. It has been revealed that the first phase is divided into two sub-phases; the 1a-phase, where most of the anomalously large output energy is produced with a very high loading, D/Pd $\approx$ 1.2, and the 1b-phase, where much smaller power is produced as loading increases further by a ratio of about 0.5 with a difference in pressure between deuterium and hydrogen.
© 2011 ISCMNS. All rights reserved.

Keywords: D/Pd loading ratio, Heat output, Pd·Zr oxide compounds, Time-resolved measurements, Two sub-phases

1. Introduction

The present work describes experiments on deuterium gas charging of palladium nano-powders in the form of Pd/ZrO_2 nano-composite. This work is a replication of Arata and Zhang [1], which was in turn a sophisticated, yet simplified, version of the Arata and Zhang's previous-generation experiments with double-structured reactors [2]. With the new configuration, Arata and Zhang report anomalous heat and helium-4 generation. If confirmed, this would be an extremely important phenomenon, so it is crucial that it be replicated if possible. Although successful replications using systems similar to the original double-structured reactor with Pd-black have been reported [3,4], few reports of replications of heat and helium-4 with the new configuration have been published.

We constructed an experimental system to replicate the phenomenon and to investigate the underlying physics [5,6]. The system is composed of two identical reaction chambers, what we call a "twin system" where the chambers

*E-mail: kitamura@maritime.kobe-u.ac.jp

© 2011 ISCMNS. All rights reserved.

are designated A_1 and A_2. Both chambers are equipped for calorimetry. A third chamber, designated B, is equipped for nuclear diagnostics. We have performed heat measurements as well as charged particle measurements under D_2 or H_2 absorption by a variety of palladium nano-powders [5–16] including: 0.1-μmϕ Pd powder (PP); 300-mesh Pd-black (PB); oxide composites of Pd·Zr (PZ); oxide composites of Pd·Ni·Zr (PNZ) and oxide composites of Ni·Zr (NZ). We have recently reevaluated the loading ratios D/Pd (or H/Pd) and E_1 based on a revised value for the volume of the of the reaction chamber, which we now estimate is 120 ml. The revised results are as follows:

(a) The loading ratio D/Pd $\approx$ 0.44 (H/Pd is also $\sim$0.44) and the first phase absorption energy $E_1 \approx 0.26$ eV/atom-D (or 0.20 for H) for the PP samples. These figures are in good agreement with those found in the literature [17–22]. The figures for both deuterium and hydrogen increase as a function of the fineness of the sample surface, where the PP samples have the roughest surface, followed by PB, and PZ is the finest.

(b) For the virgin PB samples, the loading ratios for both D/Pd and H/Pd = 1.3 ± 0.04 and the output energies in the first phase, $E_1 = 0.42 \pm 0.07$ eV/atom-D (or 0.39 for H). These values are 2–3 times larger than for the PP sample.

(c) The virgin PZ samples have shown outstanding performance with very high loading ratios D/Pd = 1.8 ± 0.3 (or 1.7 H/Pd) together with the high absorption energies E_1, or the deuteride (hydride) formation energy $Q_{D(H)}$ ranging from 0.92 to 1.4 eV/D (and 0.92–1.2 eV/H) depending on how much fraction of PdO_x reduction contributes to the measured values of D(H)/Pd and E_1.

(d) The PB and PZ samples have given substantially smaller D/Pd (and H/Pd) ratios and E_1 values in their recycled use. These are smaller than or nearly equal to those for the PP samples. We inferred that these are due to a clumping-together (aggregation) effect of palladium nano-particles.

(e) The outstanding performances of the PZ sample have been significantly restored by oxidizing a small amount (less than 10%) of the sample. The runs after forced oxidization allowed us to measure the hydridation energy, $Q_{D(H)} = 1.11 \pm 0.04$ eV/D (0.93 ± 0.09 eV/H), which is about 2 times larger than the adsorption energy, and 5 times larger than the absorption energy of a bulk-Pd-metal.

(f) In the second phase, we observed positive output, $E_2 \sim 2.5$ kJ/g-Pd for the deuterium runs employing both the virgin PZ and the used-PZ samples and the PNZ sample. However, this was only slightly above the margin of error, so it will have to be confirmed in further investigation.

In these experiments, we determined the amount of hydrogen isotopes absorbed/adsorbed by the samples of palladium from the gas flow rate multiplied by the duration of the first phase, with the gas flow rate being calculated from a rate of the pressure increase in the reaction chamber at the beginning of the second phase. This determination is reasonable if absorption ends completely when the second phase begins. Otherwise, D(H)/Pd will be underestimated.

In recent tests we have improved the experimental setup by equipping the sub-tanks with pressure gauges to directly measure the flow rate and the loading ratio [16]. Deuterium (or hydrogen) gas is stored in this sub-tank beforehand, and then absorption runs are initiated after closing the gas supply-valve on the head of the gas cylinder to close the system. With this improvement, we can make accurate time-resolved measurements of absorbed amount of gas as well as the flow rate. This enables a measurement of time-dependent sorption energy for each hydrogen isotope (differential heat of hydrogen uptake), which we describe in the present paper.

2. Experimental Procedure

The D_2/H_2 absorption system is composed of two identical chambers (A_1·A_2 twin system): one for a D_2 gas foreground run, and the other for an H_2 gas background run. As shown in Fig. 1, each of the twin systems has an inner reaction chamber containing palladium powder and an outer chamber that is evacuated to provide thermal insulation for calorimetry. The detailed description of the system is given in refs. [14,16]. The statistical error in the output power is

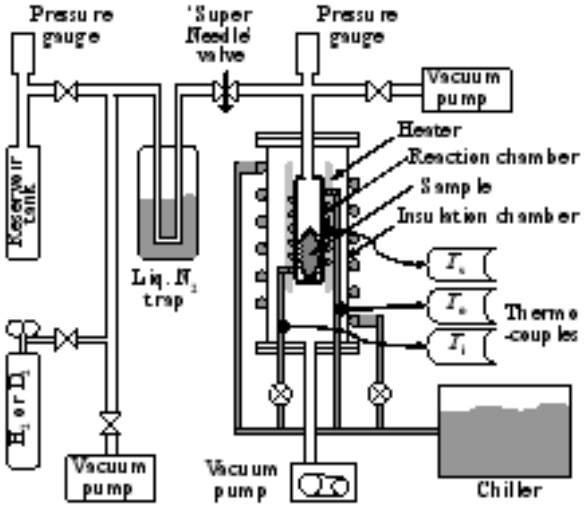

Figure 1. Schematic of one of the twin absorption systems.

evaluated based on the standard deviation of the longitudinal data, and is 0.67 mW. This is multiplied by the duration of the first phase to give the statistical error in the time-integrated output energy, e.g., 4.0 kJ for a 100-min run.

The data nomenclature is as follows. The run number is designated G-PN#M(A)(d), where G is the gas species (D or H); P the type of powder (PP, PB, PZ); N the powder identification number; and M the number of times the powder has been used. The number M is incremented when a sample is baked and then used in another absorption run. When the sample is reused without baking it, in what might be considered a continuation of the same run, the number M is not incremented. The letter A, B, or C is appended to the number instead. Thus, D-PZ11#3B indicates a run with deuterium, a PZ powder, powder identification number 11, which has been baked and run 3 times, and then run again without baking (run 3B).

Every absorption run is followed by a desorption run, which is carried out by evacuating the reaction chamber. This is an endothermic process. The thermal data has occasionally been processed and presented in the data tables with the run designation lower-case "d." For the example above, data from a desorption run following the 3B absorption run would be labeled DPZ11#3Bd.

The powder species used in the present paper are mixed oxides of Pd·Zr (PZ) fabricated by Santoku Corporation, Kobe, Japan.

To analyze the heat evolution, we assume that the chemical reaction that occurs during loading is described in Eq. (1) or Eq.. (2). These describe a combination of an oxygen pickup reaction during the formation of D_2O (or H_2O) with a reduction energy of Q_{red} (expressed as eV/atom-Pd) and a hydridation reaction during the formation of hydride atoms PdD(H) and surface adatoms with a reaction energy of $Q_{\mathrm{D(H)}}$ (eV/atom-D(H)).

$$\mathrm{PdO}_x + \left(x + \frac{y}{2}\right)\mathrm{D}_2 = x\mathrm{D}_2\mathrm{O} + \mathrm{PdD}_y, \tag{1}$$

$$\mathrm{PdO}_x + \left(x + \frac{y}{2}\right)\mathrm{H}_2 = x\mathrm{H}_2\mathrm{O} + \mathrm{PdH}_y. \tag{2}$$

Here a fraction x of Pd is assumed to have been oxidized and reduced by introduction of D_2 (H_2), while a fraction y of Pd is deuterized (or hydrized).

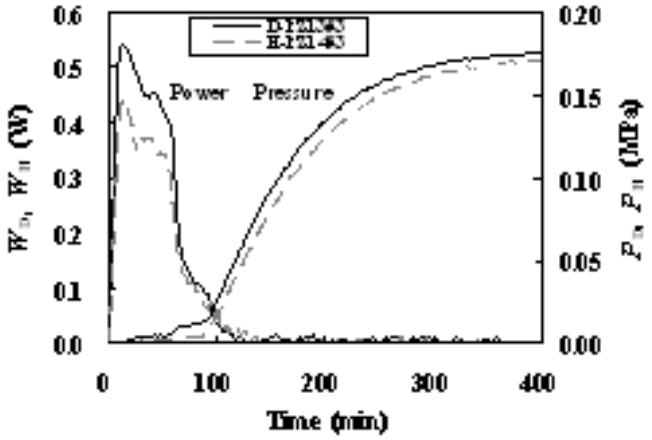

Figure 2. Typical variation of output power, W_D and W_H, and pressure in the reaction chamber, P_D and P_H.

The specific output energy, E_1 either in units of (kJ/g-Pd) or (eV/atom-Pd) is expressed as

$$E_1 = x\,Q_{\mathrm{red}} + y\,Q_{\mathrm{D(H)}}. \tag{3}$$

The fraction y and the energy $Q_{\mathrm{D(H)}}$ may include those of bulk hydride formation and adsorption to the palladium particle surface as well as other possible reactions. We take the value of Q_{red} = 1.85 eV/atom-Pd (or 1.68 for H) from the literature.

The value of y is calculated from the mass conservation law during the gas introduction through the Super Needle:

$$\frac{P_{\mathrm{R0}}V_{\mathrm{R}}}{N_{\mathrm{A}}kT_{\mathrm{R}}} = \frac{P_{\mathrm{R}}V_{\mathrm{R}}}{N_{\mathrm{A}}kT_{\mathrm{R}}} + \frac{PV}{N_{\mathrm{A}}kT} + \left(\ell x + \frac{y}{2}\right), \tag{4}$$

where (V_{R}, P_{R}) and (V, P) are the (volume, pressure) of the upstream (reservoir) tank and the downstream (reaction) chamber subdivided by the Super Needle, respectively, both including the connecting pipes. The left-hand side of Eq. (4) represents the amount (in mol) of D_2 (H_2) molecules in the reservoir tank before opening the Super Needle, and λ represents the fraction of liquid D_2O (H_2O), if any, generated as a result of the reduction. The third term on the right-hand side of Eq. (4) then represents the volume (in mol) of D_2 (H_2) molecules lost to liquefaction or absorption/adsorption. In the present experimental conditions it is assumed that the water molecules produced through the reaction (1) will remain in the gas phase, i.e., $\lambda = 0$.

To see the effect of oxygen, the sample was occasionally oxidized or deoxidized deliberately [14,16]. The value of x is calculated from the pressure decrease during the oxidization process.

3. Experimental Results and Discussion

3.1. Time integrated parameters in absorption/desorption runs for PZ samples

Typical variations of the output power, W_D and W_H, after the introduction of D_2 and H_2 gas are shown in Fig. 2 together with the pressure, P_D and P_H, in each reaction chamber for the PZ13 and PZ14 samples. As seen in the other runs described above, the pressure remains low during the main heat generation period, which we call the first phase.

In the absence of an apparent anomaly, the first phase heat is dominated by the chemical reaction of absorption and adsorption. In some cases, we have observed positive output in the second phase. In the runs described here, however, we observed no significant output, even when the reservoir pressure was increased to 1 MPa.

Table 1 and Fig. 3, which show the same results described in [16], summarize the parameters integrated over the first phase of the runs using PZ11 through PZ14; the specific output energy E_1 in units of both kJ/g-Pd and eV/atom-Pd, which is the time-integrated output power per palladium atom; the loading ratio y_D (y_H) at the end of the first phase, which is calculated from Eq. (4); and the hydridation energy calculated with Eq. (3). Here it is assumed that the water molecules produced through the reaction (1) will remain in the gas phase, i.e., $\lambda = 0$.

The results are briefly summarized as follows. The virgin PZ samples (No. 1 runs) have very large specific output energy, $E_1 = 2.28 \pm 0.42$ eV/atom-Pd for D-runs or $E_1 = 2.28 \pm 0.29$ eV/atom-Pd for H-runs on average, as well as very high loading ratios, D/Pd =2.31 ± 0.06 or H/Pd = 2.29 ± 0.03.

The specific energy E_1 for these "recycle" runs is more than one order of magnitude smaller than the virgin runs. The loading ratios, D/Pd and H/Pd, also decrease for the recycle runs to average values of 0.60 ± 0.10 and 0.49 ± 0.14 (by a factor of about 4), respectively. Accordingly, the hydridation energy $Q_{D(H)}$ also decreases for the recycle runs to average values of 0.27 ± 0.02 eV/D (0.30 ± 0.08 eV/H) (by a factor of about 3), respectively. These are consistent with those for the bulk (PP) samples.

We see essentially the same values for E_1, D/Pd (or H/Pd) and Q_D (or Q_H) in the No. 2 (deoxidized sample) runs as those in the recycle runs. However, the performance characteristics are largely recovered in the No. 3 runs by oxidizing the sample palladium to a small extent (a few percent). The averaged values are: E_1 =1.97 ± 0.1 eV/Pd, D/Pd = 1.72 ± 0.09 and Q_D =1.11 ± 0.04 eV/D for D-runs, and $E_1 = 1.37 \pm 0.06$ eV/Pd, H/Pd = 1.44 ± 0.16 and $Q_H = 0.93 \pm 0.09$ eV/H for H-runs. A detailed discussion of these results is found in [16].

3.2. Time-resolved parameters; loading ratio and specific absorption energy

Since we were monitoring the time-dependent pressure both in the reaction chamber and the reservoir tank constituting a closed system, we can calculate time-resolved loading ratio D(H)/Pd, defined as $L_{D(H)}(t)$, which is equal to the parameter $y_{D(H)}$ defined in Eq. (1), when we can assume that the water molecules, if any, have negligible volume, i.e., $\lambda = 0$.

Figure 4 shows $L_{D(H)}(t)$ as a function of pressure $P_{D(H)}$ in the first phase for D(H)-PZ13(14)No. 1, D(H)-PZ13(14)No. 2 and D(H)-PZ13(14)No. 3 runs. This relationship between the pressure and the loading ratio corresponds roughly to the absorption isotherm, since the temperature change during the run is smaller than a few degrees Celsius. We find a similarity between the traces for the No. 1 run (a) and the No. 3 run (c). In both cases there are two distinct phases, phase 1a and phase 1b. In phase 1a the choice of isotopes, deuterium or hydrogen, has no effect, while in phase 1b deuterium produces higher pressure.

The transition from the 1a-phase to the 1b-phase occurs at about 60 min for the No. 3 run, which is readily apparent in Fig. 2. The effect of the isotopes (deuterium or hydrogen) appears to be of the same nature as that in [24]. The pressure during the 1b-phase for the D-runs is about 10 kPa, while that for the H-runs it is about 5 kPa. Note that the No. 2 run has only the 1b-phase. The hydrogen uptake in the 1b-phase is $\Delta L_{D(H)} \approx 0.5$ in all cases. These values of the pressure and the hydrogen uptake are consistent with those extrapolated from the values found in ref. [24] which used 10-μm-thick palladium foils. From this we infer that the 1b-phase is characteristic of the bulk palladium absorption, and not of the surface adsorption. On the other hand, the 1a-phase is considered to be characteristic of the sample containing PdO, since the samples for the No. 2 runs have no oxygen.

From the above results we can exclude the possibility that the anomalously large D(H)/Pd might be due to condensation of D_2O (or H_2O) atoms into the liquid phase with negligible volume, i.e., an overestimation of D(H)/Pd (= y) due to a nonzero λ (cf. Eq. (4)). Condensation, if it could occur, would be in the 1b-phase at higher pressure. However, the

Table 1. Summary of the first phase parameters in absorption/desorption runs for PZ11 through PZ14 samples. Contribution of deoxidization (oxygen pick-up and water formation) to the output energy is not subtracted in calculating $Q_{D(H)}$ in the case of the virgin sample runs indicated with asterisks*.

Run No.	O/Pd (= x)	Specific output energy E_1 (kJ/g-Pd)	Specific output energy E_1 (eV/atom-Pd)	D/Pd(= y)	Q_D (eV/D)	Remarks
D-PZ11						
No. 1	Unknown	1.69 ± 0.05	1.86	2.37	0.79*	Virgin
No. 2	0	0.14± 0.01	0.16	0.56	0.28	Deoxidized
No. 3	0.086	1.88 ± 0.07	2.08	1.81	1.15	Oxidized
No. 3d	0	–0.13 ± 0.01	–0.14	–	–	
No. 3A	0	0.14 ± 0.01	0.15	0.56	0.27	
No. 3Ad	0	–0.11 ± 0.01	–0.12	–	-	
No. 3B	0	0.12 ± 0.01	0.14	0.49	0.28	
No. 3Bd	0	–0.11 ± 0.01	–0.13	–	–	
D-PZ13						
No. 1	Unknown	2.44 ± 0.13	2.69	2.25	1.20*	Virgin
No. 1d	0	–0.27 ± 0.03	–0.30	–	–	
No. 1A	0	0.16 ± 0.02	0.18	0.63	0.28	
No. 1Ad	0	–0.16 ± 0.02	–0.18	–	–	
No. 1B	0	0.15 ± 0.01	0.16	0.70	0.23	
No. 1Bd	0	–0.14 ± 0.01	–0.16	–	–	
No. 2	0	0.26 ± 0.06	0.23	0.59	0.39	Deoxidized
No. 2d	0	–0.17 ± 0.02	–0.18	–	–	
No. 3	0.073	1.69 ± 0.17	1.87	1.63	1.06	Oxidized
H-PZ12						
No. 1	Unknown	1.80 ± 0.13	1.99	2.26	0.88*	Virgin
No. 2	0	0.14 ± 0.01	0.16	0.45	0.35	Deoxidized
No. 3	0.054	1.18 ± 0.05	1.31	1.28	1.02	Oxidized
No. 3d	0	–0.10 ± 0.01	–0.11	–	–	
No. 3A	0	0.11 ± 0.01	0.12	0.41	0.29	
No. 3Ad	0	–0.10 ± 0.01	–0.11	–	–	
No. 3B	0	0.10 ± 0.01	0.11	0.44	0.25	
No. 3Bd	0	–0.09 ± 0.01	–0.10	–	–	
H-PZ14						
No. 1	Unknown	2.32 ± 0.12	2.56	2.31	1.11*	Virgin
No. 1d	0	–0.42 ± 0.05	–0.46	–	–	
No. 1A	0	0.13 ± 0.01	0.15	0.35	0.42	
No. 1Ad	0	–0.16 ± 0.02	–0.18	–	–	
No. 1B	0	0.16 ± 0.02	0.18	0.73	0.25	
No. 1Bd	0	–0.16 ± 0.02	–0.18	–	–	
No. 2	0	0.19 ± 0.04	0.21	0.65	0.33	Deoxidized
No. 2d	0	–0.14 ± 0.01	–0.22	–	–	
No. 3	0.061	1.29 ± 0.13	1.43	1.59	0.83	Oxidized

1b-phase is observed also in the No. 2 runs with no oxygen involved. Therefore, it is unlikely we have overestimated D(H)/Pd because of condensation.

We can define time-resolved specific sorption energy, or differential heat of hydrogen uptake, $\eta_{D(H)}(t)$, as the output energy per hydrogen isotope atom absorbed/adsorbed, which is calculated as the output energy during a time interval

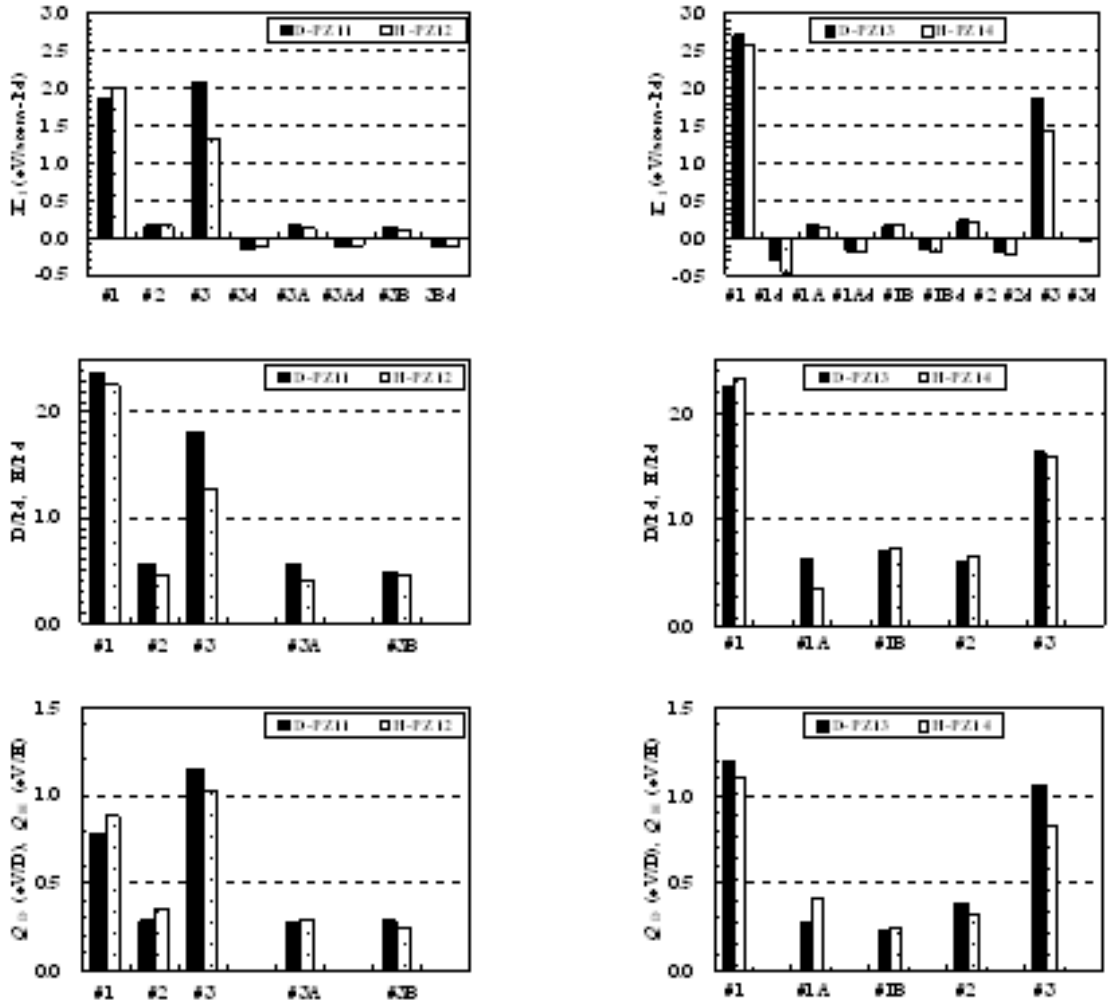

Figure 3. First phase parameters in comparison with D-runs and H-runs; specific output energy E_1, loading ratio D(H)/Pd, and hydridation energy $Q_{\mathrm{D(H)}}$.

τ divided by the increment of $L(t)$ in the same interval;

$$\eta(t) \equiv \frac{\int_t^{t+\tau} W_{\mathrm{s}}(t)\mathrm{d}t}{L(t+\tau) - L(t)}, \tag{5}$$

where $W_{\mathrm{s}}(t)$ is in unit of power per palladium atom including the contribution from the oxygen pickup reaction. The interval τ is arbitrary, and chosen here to be the time constant of the calorimetry system. For the samples with no oxygen involved, the hydridation energy $Q_{\mathrm{D(H)}}$ introduced above is equal to time-averaged value of $\eta_{\mathrm{D(H)}}(t)$ with τ being the first phase duration and $t = 0$. Since both $W_{\mathrm{s}}(t)$ and $L(t)$ are values per palladium (absorber) atom, $\eta_{\mathrm{D(H)}}(t)$ is independent of sample constituent, namely whether we use PZ or PNZ or other mixed samples.

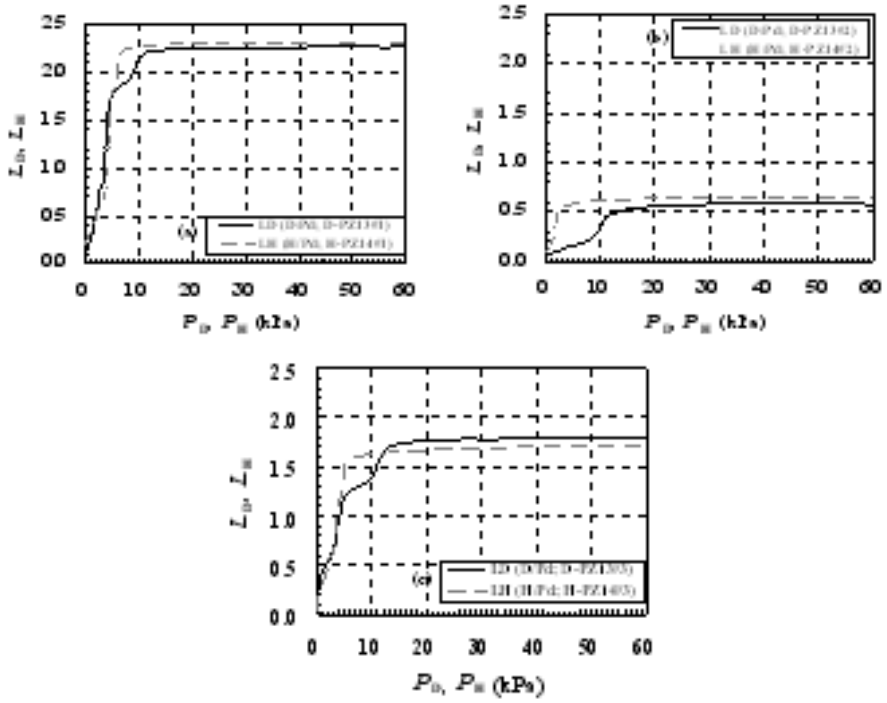

Figure 4. Time-resolved loading ratio, L_D and L_H, expressed as a function of pressure in PZ13(14)No. 1–3 runs. The first phase appears to be divided into 1a-phase and 1b-phase.

Figure 5 shows examples of time-resolved sorption energy $\eta_{D(H)}$ and loading ratio $L_{D(H)}$ compared with the output power $W_{D(H)}$ in the run D(H)–PZ13(14)No. 3. We notice here again that the evolution of heat has two phases divided at t = 60 min. The heat evolution associated with hydrogen isotope absorption/adsorption proceeds mainly in the low-pressure 1a-phase below ∼4 kPa. In a difference from $L_{D(H)}(t)$, a not-inconsiderable difference in the effect of the isotopes (deuterium or hydrogen) is observed for the heat evolution in the 1a-phase: $\eta_D \approx 1.33$ eV/D, while $\eta_H \approx 1.15$ eV/H. On the other hand, a relatively small amount of heat is generated in the 1b-phase from 60 to 100 min; $\eta_D \approx 0.47$ eV/D and $\eta_H \approx 0.41$ eV/H with a moderate isotope effect compared with that in the pressure mentioned above.

It has been found that most of the heat evolution from the samples in the 1a-phase only occurs when oxygen atoms are involved, and the 1b-phase with no oxygen produces much less heat. From this we might infer that the main heat source is the oxygen pickup reaction. However, it must be emphasized that $Q_{D(H)}$ obtained after the contribution of the deoxidization subtracted from E_1 is still anomalously large, being 1.11 ± 0.04 eV/D (or 0.93 ± 0.09 eV/H), as was shown in Table 1 and Fig. 3. Therefore, the main heat source in the 1a-phase is related to the presence of oxygen, but it is independent of the deoxidization reaction. From the fact that the 1a-phase proceeds at low pressure with little difference in the effect of the isotopes (deuterium or hydrogen) on pressure, we conclude that the heat source is on or near the surface of palladium nanoparticles, or that the reaction is triggered on or near the surface.

What is important is that the hydridation energy $Q_{D(H)}$ = 1.11 ± 0.04 (0.93 ± 0.09) eV/D(H) is much larger than the bulk hydride formation energy (≅ 0.2 eV) and the surface adsorption energy (≅ 0.5 eV). Huang et al. [23] have reported that differential heat of hydrogen uptake for hydrogen chemisorption reaches or even exceeds 1 eV/H for a

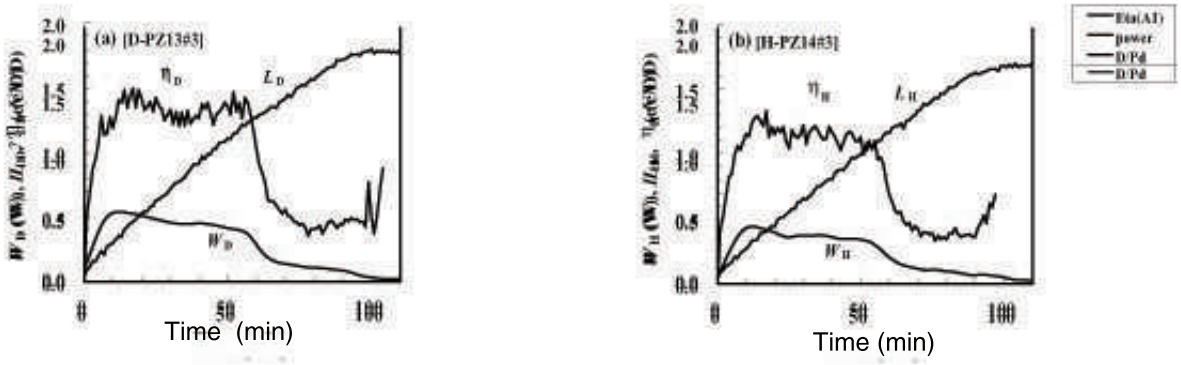

Figure 5. Time-resolved sorption energy $\eta_{D(H)}$, loading ratio $L_{D(H)}$ compared with the output power $W_{D(H)}$ in the run D(H)-PZ13(14)No. 3.

dispersed 2-nm-diameter palladium particles. In the present case of our Santoku samples, however, the mean diameter of the palladium nanoparticles is 10 nm, and oxygen incorporation is necessary for the large hydridation energy.

A phenomenological modeling and discussions on the role of the PdO layer of the Pd-nano-particle and possible mechanisms relating the anomalous heat component found in the present work to a nuclear origin are given in the separate papers [15, 25]

4. Conclusion

The hydrogen isotope absorption/adsorption system has been improved to enable time-dependent measurements of the gas flow rate and the D (or H) loading ratio simultaneously with the thermal output power. Runs using the samples after forced deoxidization and forced oxidization, as well as the virgin runs at room temperature, have revealed interesting facts. The first phase, in which chemical heat is produced, is divided into two subphases, after which the chemical heat is completed. In the 1a-phase, the predominant heat evolution is associated with hydrogen isotope absorption/adsorption, and proceeds under relatively low pressure below about 4 kPa with the specific sorption energy being $\eta_D \approx 1.33$ eV/D and $\eta_H \approx 1.15$ eV/H. In the 1b-phase, a relatively small amount of heat is generated under an isotope-dependent pressure of several to 10 kPa with $\eta_D \approx 0.47$ eV/D and $\eta_H \approx 0.41$ eV/H. It should be noted that samples tested after forced deoxidization exhibited only the 1b-phase. The 1a-phase only appears with samples incorporating oxygen.

References

[1] Y. Arata, Y. Zhang, The establishment of solid nuclear fusion reactor, *J. High Temperature Soc*. **34**(2) (2008) 85–93.
[2] Y. Arata, Y. Zhang, *Condensed Matter Nuclear Science*, *Proc. 12th Int. Conf. on Cold Fusion*, A. Takahashi, Y. Iwamura, K. Ota (eds.), World Scientific, Singapore, 2006, pp. 44–54.
[3] V.A. Kirkinskii, A.I. Kumelnikov, *Proc. ICCF13, Sochi,* Publisher Center MATI, Moscow, ISBN 978-5-93271-428-7, 2007, pp. 43–46.
[4] J.P. Biberian, N. Armanet, *ibid*. pp. 170–180.
[5] T. Nohmi, Y. Sasaki, T. Yamaguchi, A. Taniike, A. Kitamura, A. Takahashi, R. Seto, Y. Fujita, http://www.ler-canr.org; to be published in *Proc. 14th Int. Conf. Condensed Matter Nuclear Science (ICCF14)*, Washington, DC, 2008.
[6] Y. Sasaki, A. Kitamura, T. Nohmi, Y. Miyoshi, A. Taniike, A. Takahashi, R. Seto, Y. Fujita, *Proc. 9th Meeting of Japan CF-Research Society*, 2009, pp. 29–34; http://www.lenr-canr.org/acrobat/SasakiYdeuteriumg.pdf.
[7] A. Takahashi, A. Kitamura, T. Nohmi, Y. Sasaki, Y. Miyoshi, A. Taniike, R. Seto, Y. Fujita, *ibid.* pp. 35–41; http://www.lenr-canr.org/acrobat/TakahashiAdeuteriumg.pdf.

[8] A. Kitamura, T. Nohmi, Y. Sasaki, A. Taniike, A. Takahashi, R. Seto, Y. Fujita, *Phys. Lett.* A **373** (2009) 3109–3112.
[9] Y. Sasaki, A. Kitamura, Y. Miyoshi, T. Nohmi, A. Taniike, A. Takahashi, R. Seto, Y. Fujita, to be published in *Proc. 15th Int. Conf. Condensed Matter Nuclear Science (ICCF15)*, Rome, 2009; http://iccf15.frascati.enea.it/ICCF15-PRESENTATIONS/S7_O5_Sasaki.pdf.
[10] A. Takahashi, A. Kitamura, Y. Sasaki, T. Miyoshi, T. Nohmi, A. Taniike, Y. Furuyama, R. Seto, Y. Fujita, *ibid*., */S2_O4_Takahashi.pdf*.
[11] A. Kitamura, Y. Sasaki, Y. Miyoshi, T. Nohmi, T. Yamaguchi, A. Taniike, Y. Furuyama, A. Takahashi, R. Seto, Y. Fujita, *ibid*., */S3_O2_Kitamura.pdf*.
[12] A. Kitamura, A. Takahashi, Y. Sasaki, Y. Miyoshi, A. Taniike, R. Seto, Y. Fujita, to be published in *J. Condensed Matter Nucl. Sci.*
[13] Y. Sasaki, Y. Miyoshi, A. Taniike, A. Kitamura, A. Takahashi, R. Seto, Y. Fujita, Measurements of heat and radiation from Pd nano-powders during absorption of hydrogen isotopes, *Proceedings of JCF10 Meeting*, Japan CF-Research Society, 2010, paper JCF10-3.
[14] Y. Miyoshi, Y. Sasaki, A. Taniike, A. Kitamura, A. Takahashi, R. Seto, Y. Fujita, Absorption/adsorption processes of hydrogen isotopes observed for Pd nano-powders, *ibid*., paper JCF10-4.
[15] A. Takahashi, A. Kitamura, Y. Sasaki, Y. Miyoshi, A. Taniike, R. Seto, Y. Fujita, Role of PdO Surface-Coating of Pd Nano-Particle for D(H) Charging and Cluster Fusion, *ibid*., paper JCF10-5.
[16] A. Kitamura, Y. Miyoshi, H. Sakoh, A. Taniike, A. Takahashi, R. Seto, Y. Fujita, Anomalous heat evolution in charging of Pd nano-powders with hydrogen isotopes, submitted to *LENR-NET Source book 3, ACS*, J. Marwan (ed.)
[17] G. Alefeld, J. Voelkl (eds.), *Hydrogen in Metals II–Topics in Applied Physics*, vol. 29, Springer, Berlin, 1978.
[18] A Koiwai, A. Itoh, T. Hioki, Japan Patent 2005-21860 (P2005-21860A).
[19] C.P. Chang et al., *Int. J. Hydrogen Energy* **16** (1991) 491.
[20] M.M. Antonova, *Sboistva Gidriedov Metallov (Properties of Metal-hydrides)*, Naukova Dumka, Kiev, 1975; translated by NissoTsushinsha, Wakayama, 1976 [in Japanese].
[21] Y. Fukai, K. Tanaka, H. Uchida, *Hydrogen and Metals*, Uchida Rokakuho, Tokyo, 1998 [in Japanese].
[22] P. Chou, M.A. Vannice, *J. Catalysis* **104** (1987) 1–16.
[23] S.-Y. Huang, C.-D. Huang, B.-T. Chang, C.-T. Yeh, *J. Phys. Chem.* B **110** (2006) 21783–21787.
[24] R. Laesser, K.-H. Klatt, *Phys. Rev.* B **28** (1983) 748–758.
[25] A. Takahashi, A. Kitamura, Y. Sasaki, Y. Miyoshi, A. Taniike, R. Seto, Y. Fujita, Phenomenological Model on the Role of PdO Surface-Coating in CMNE D(H)-Gas Loading Experiments, to be published in *J. Condensed Matter Nucl. Sci.*.